

Late internal-shock model for bright X-ray flares in gamma-ray burst afterglows and GRB 011121

Y. Z. Fan^{1,2,3★} and D. M. Wei^{1,2★}

¹*Purple Mountain Observatory, Chinese Academy of Science, Nanjing 210008, China*

²*National Astronomical Observatories, Chinese Academy of Sciences, Beijing 100012, China*

³*Department of Physics, University of Nevada, Las Vegas, NV 89154, USA*

Accepted 2005 September 1. Received 2005 August 31; in original form 2005 May 19

ABSTRACT

We explore two possible models which might give rise to bright X-ray flares in gamma-ray burst (GRB) afterglows. One is an external forward-reverse shock model, in which the shock parameters of forward-reverse shocks are taken to be quite different. The other is a so-called ‘late internal-shock model’, which requires a refreshed unsteady relativistic outflow generated after the prompt γ -ray emission. In the forward-reverse shock model, after the time t_{\times} at which the reverse shock crosses the ejecta, the flux declines more slowly than $(t_{\oplus}/t_{\times})^{-(2+\beta)}$, where t_{\oplus} denotes the observer’s time and β is the spectral index of the X-ray emission. In the ‘late internal-shock model’, decaying slopes much steeper than $(t_{\oplus}/t_{e,\oplus})^{-(2+\beta)}$ are possible if the central engine shuts down after $t_{e,\oplus}$ and the observed variability time-scale of the X-ray flare is much shorter than $t_{e,\oplus}$.

The sharp decline of the X-ray flares detected in GRB 011121, XRF 050406, GRB 050502b and GRB 050730 rules out the external forward-reverse shock model directly and favours the ‘late internal-shock model’. These X-ray flares could thus hint that the central engine has begun to operate again and a new unsteady relativistic outflow is generated just a few minutes after the intrinsic hard burst.

Key words: radiation mechanisms: non-thermal – ISM: jets and outflows – gamma-rays: bursts – X-rays: general.

1 INTRODUCTION

GRB 011121 was simultaneously detected by *BeppoSAX* GRBM and WFC (Piro 2001), and the fluence in the 2–700 keV range corresponds to an isotropic energy of 2.8×10^{52} erg at a redshift of $z = 0.36$ (Infante et al. 2001). This burst was born in a stellar wind (Price et al. 2002; Greiner et al. 2003) and a supernova bump was detected in the late optical afterglow (Bloom et al. 2002; Garnavich et al. 2003). Its very early X-ray light curve, which has not been published until quite recently, is characterized by the presence of two flares (Piro 2005, hereafter P05). In the first flare, which is also the strongest of the two, the observed flux F rises and decays very steeply: $F \propto t_{\oplus}^{10}$ for $239 \text{ s} < t_{\oplus} < 270 \text{ s}$ and $F \propto t_{\oplus}^{-7}$ for $270 \text{ s} < t_{\oplus} < 400 \text{ s}$, where t_{\oplus} is the observer’s time.¹ Such a peculiar flare in the early X-ray light curve of gamma-ray bursts (GRBs) has not been predicted before. P05 suggested that the X-ray flare (XRF) represents the beginning of the afterglow.

★E-mail: yzfan@pmo.ac.cn (YZF); dmwei@pmo.ac.cn (DMW)

¹ During our revision, bright X-ray flares peaking a few minutes after XRF 050406, GRB 050502b and GRB 050730 have been reported (Burrows et al. 2005; Starling et al. 2005). Sharp rises and falls are also evident in these events.

In this Letter we explore two alternative models which might give rise to very early X-ray flare in GRB afterglows (Section 2): a forward-reverse shock model (Section 2.1) and a ‘late internal-shock model’ (Section 2.2). We compare the available data with the predictions of those models in Section 3 and summarize our results in Section 4, with some discussion.

2 POSSIBLE MODELS

2.1 The external forward-reverse shock model

The external forward-reverse shock model has been widely accepted as an interpretation of the early IR/optical flashes of GRB 990123, GRB 021211 and GRB 041219a. (For observations, see Akerlof et al. 1999; Fox et al. 2003; Li et al. 2003 and Blake et al. 2005. For theoretical modelling, see Sari & Piran 1999; Mészáros & Rees 1999; Wei 2003; Kumar & Panaitescu 2003 and Fan, Zhang & Wei 2005). Synchrotron radiation from the reverse shock (RS) and the forward shock (FS) usually peaks in the infrared-to-optical and ultraviolet-to-soft-X-ray bands, respectively. Thus, the RS emission component is not dominant in the X-ray band. The synchrotron self-Compton (SSC) scattering effect of the RS radiation has also been considered by different authors, but no strong X-ray emission has

been found to be expected (Wang, Dai & Lu 2001) except in some carefully balanced conditions (Kobayashi et al. 2005).

In most previous works, the fractions of FS energy given to electrons, ϵ_e , and to magnetic field, ϵ_B , were assumed to be the same as the corresponding fractions in the RS. However, this may not necessarily be the case. Fan et al. (2002) performed a detailed fit to the optical flash of GRB 990123 data and obtained $\epsilon_e^r = 4.7\epsilon_e^f$ and $\epsilon_B^r = 400\epsilon_B^f$ where the superscripts ‘r’ and ‘f’ represent RS and FS, respectively. Similar results were obtained by Zhang, Kobayashi & Mészáros (2003), Kumar & Panaitescu (2003), Panaitescu & Kumar (2004), McMahon, Kumar & Panaitescu (2004), and Fan et al. (2005). In this section, we study the RS/FS emission in the X-ray band by adopting different shock parameters. We focus on the thin-shell case (i.e. the RS is sub-relativistic, see Kobayashi 2000), in which the RS emission is well separated from the prompt γ -ray emission.

ISM model. In the thin-shell case, the observer’s time at which RS crosses the ejecta can be estimated by (e.g. Fan et al. 2005)

$$t_x \approx 128s \left(\frac{1+z}{2} \right) E_{\text{iso},53}^{1/3} n_0^{-1/3} \eta_{2.3}^{-8/3}, \quad (1)$$

where E_{iso} is the isotropic energy of the outflow, n is the typical number density of ISM, and η is the initial Lorentz factor of the outflow. The convention $Q_y = Q/10^y$ has been adopted in cgs units throughout the text except for some special notations.

In the standard afterglow model of a fireball interacting with a constant density medium (e.g. Sari, Piran & Narayan 1998), the cooling frequency $\nu_{c,\oplus}^f$, the typical synchrotron frequency $\nu_{m,\oplus}^f$, and the maximum spectral flux $F_{\nu,\text{max}}^f$ read:

$$\begin{aligned} \nu_{c,\oplus}^f &= 4.4 \times 10^{17} \text{ Hz } E_{\text{iso},53}^{-1/2} \epsilon_{B,-3}^{-3/2} n_0^{-1} t_{d,-3}^{-1/2} \\ &\quad \times \left(\frac{2}{1+z} \right) (1+Y^f)^{-2}, \\ \nu_{m,\oplus}^f &= 4.4 \times 10^{15} \text{ Hz } E_{\text{iso},53}^{1/2} \epsilon_{B,-3}^{1/2} \epsilon_{e,-1}^{-2} t_{d,-3}^{-3/2} C_p^2 \left(\frac{2}{1+z} \right), \end{aligned}$$

and

$$F_{\nu,\text{max}}^f = 2.6 \text{ mJy } E_{\text{iso},53}^{1/2} \epsilon_{B,-3}^{1/2} n_0^{1/2} D_{L,28.34}^{-2} \left(\frac{1+z}{2} \right),$$

where $C_p = 13(p-2)/[3(p-1)]$, $p \sim 2.3$ is the typical power-law distribution index of the electrons accelerated by FS,

$$Y^f \simeq [-1 + \sqrt{1 + 4x^f \epsilon_e^f / \epsilon_B^f}] / 2$$

is the Compton parameter, $x^f \approx \min\{1, (\nu_{m,\oplus}^f / \nu_{c,\oplus}^f)^{(p-2)/2}\}$ (Sari & Esin 2001), and D_L is the luminosity distance for $(\Omega_M, \Omega_\Lambda, h) = (0.3, 0.7, 0.71)$. Hereafter $t = t_\oplus/(1+z)$, and t_d is in units of days.

Following Zhang et al. (2003), we take $\epsilon_e^r = \mathcal{R}_e \epsilon_e^f$ and $\epsilon_B^r = \mathcal{R}_B^2 \epsilon_B^f$. At t_x , the RS emission satisfies [see also Fan et al. (2005), note that a novel effect taken into account here is the inverse Compton cooling of the electrons]

$$\nu_{m,\oplus}^r(t_x) = \mathcal{R}_B [\mathcal{R}_e (\gamma_{34,x} - 1)]^2 \nu_{m,\oplus}^f(t_x) / (\Gamma_x - 1)^2, \quad (2)$$

$$\nu_{c,\oplus}^r(t_x) \approx \mathcal{R}_B^{-3} [(1+Y^f)/(1+Y^r)]^2 \nu_{c,\oplus}^f(t_x), \quad (3)$$

$$F_{\nu,\text{max}}^r(t_x) \approx \eta \mathcal{R}_B F_{\nu,\text{max}}^f(t_x). \quad (4)$$

where $\gamma_{34,x} \approx (\eta/\Gamma_x + \Gamma_x/\eta)/2$ is the Lorentz factor of the shocked ejecta relative to the initial one, Γ_x is the bulk Lorentz factor of the shocked ejecta at t_x , $Y^r \simeq [-1 + \sqrt{1 + 4x^r \mathcal{R}_e \epsilon_e^f / (\mathcal{R}_B^2 \epsilon_B^f)}] / 2$ is the Compton parameter and $x^r \approx \min\{1, (\nu_{m,\oplus}^r / \nu_{c,\oplus}^r)^{(p-2)/2}\}$.

If both $\nu_{c,\oplus}^r$ and $\nu_{c,\oplus}^f$ are below the observed frequency ν_\oplus , the detected flux of RS and FS emission are

$$F_{\nu_\oplus}^r(t_x) \simeq F_{\nu_{\text{max}}}^r(t_x) [\nu_{m,\oplus}^r(t_x)]^{(p-1)/2} [\nu_{c,\oplus}^r(t_x)]^{1/2} \nu_\oplus^{-p/2}, \quad (5)$$

$$F_{\nu_\oplus}^f(t_x) \simeq F_{\nu_{\text{max}}}^f(t_x) [\nu_{m,\oplus}^f(t_x)]^{(p-1)/2} [\nu_{c,\oplus}^f(t_x)]^{1/2} \nu_\oplus^{-p/2}. \quad (6)$$

$$\frac{F_{\nu_\oplus}^r(t_x)}{F_{\nu_\oplus}^f(t_x)} \approx \eta \mathcal{R}_B^{\frac{p-2}{2}} \mathcal{R}_e^{p-1} \left(\frac{\gamma_{34,x} - 1}{\Gamma_x - 1} \right)^{p-1} \left(\frac{1+Y^f}{1+Y^r} \right). \quad (7)$$

Taking $p = 2.3$ (this choice is made to match the observed slope of the X-ray flare $\beta = p/2 = 1.15$, see P05), $\Gamma_x \approx \eta/2 \sim 100$, $\epsilon_{B,-3}^f = 1$, $\epsilon_{e,-1}^f = 1$, $\mathcal{R}_B = 10$ and $\mathcal{R}_e = 5$, we have $x^f \approx 1$, $Y^f \approx (\epsilon_e/\epsilon_B)^{1/2} = 10$, $x^r \approx 0.6$, $Y^r \approx 1.2$, and $(1+Y^f)/(1+Y^r) \gg 1$, i.e. we have a larger contrast $F_{\nu_\oplus}^r(t_x)/F_{\nu_\oplus}^f(t_x)$ when the inverse Compton effect has been taken into account. With equation (7), we have $F_{\nu_\oplus}^r(t_x)/F_{\nu_\oplus}^f(t_x) \approx 5$, i.e. *in the X-ray band, the RS emission component is dominant*. For $t_\oplus > t_x$, the RS emission declines as $(t_\oplus/t_x)^{-(2+p/2)}$ because of the curvature effect (e.g. Kumar & Panaitescu 2000, hereafter KP00).² The FS emission declines as $t_\oplus^{(2-3p)/4}$ (e.g. Sari et al. 1998), so the X-ray flare lasts $\sim [F_{\nu_\oplus}^r(t_x)/F_{\nu_\oplus}^f(t_x)]^{4/(10-p)} t_x \sim 300$ s. Taking $z = 0.36$, $Q_y = 1$, and $\nu_x = 2.4 \times 10^{17}$ Hz, we have $\nu_x F_{\nu_x}^f \sim 10^{-9} \text{ erg cm}^{-2} \text{ s}^{-1} [(1+z)/1.36] D_{L,27.7}^{-2}$. The peak flux of the X-ray flare is $\simeq \nu_x [F_{\nu_x}^f + F_{\nu_x}^r] \sim 5 \times 10^{-9} \text{ erg cm}^{-2} \text{ s}^{-1} [(1+z)/1.36] D_{L,27.7}^{-2}$, which is consistent with the observation of GRB 011121 ($\sim 2.4 \times 10^{-9} \text{ erg cm}^{-2} \text{ s}^{-1}$, see P05). However, the accompanying optical flash is very bright. With the typical parameters taken here, the V band flux is ~ 5 Jy.

Wind model. GRB 011121 was born in a stellar wind. The best-fitting parameters are $p = 2.5$, $E_{\text{iso},52} = 2.8$, $A_* \sim 0.003$, $\epsilon_e^f \sim 0.01$, and $\epsilon_B^f \sim 0.5$ (P05). It is straightforward to show that with proper choice of \mathcal{R}_e and \mathcal{R}_B , at t_x , the RS emission may be dominant in the soft X-ray band.

Numerical results. Following Fan et al. (2005), the FS–RS emission (in the X-ray band) has been calculated numerically. In the ISM case (see Fig. 1a), the parameters are taken as $E_{\text{iso},53} = 1$, $p = 2.4$, $\epsilon_e^f = 0.1$, $\epsilon_B^f = 0.001$, $n = 1 \text{ cm}^{-3}$, and the initial width of the outflow $\Delta = 6 \times 10^{11} \text{ cm}$. In the wind model (see Fig. 1b), we take the best-fitting parameters presented in P05.

As shown in Fig. 1(a), in the ISM model, an X-ray flare dominated by the RS emission occurs only when both \mathcal{R}_B and \mathcal{R}_e are much larger than unity. In the wind model, with proper \mathcal{R}_B and \mathcal{R}_e , the RS emission may be dominant in the soft X-ray band, too. No flare is expected, however, since both the FS and RS emission components decrease continually even at very early times (see also Zou, Wu & Dai 2005). So the FS–RS scenario is unable to account for the X-ray flare detected in GRB 011121. Moreover, in the general framework of accounting for X-ray flares in GRB afterglows, the FS–RS model is further disfavoured because, even in an ISM scenario that has parameters suitable for a RS flare arising above the FS emission, the predicted temporal decay is too shallow when compared to the steep decay of X-ray flares observed so far (see Fig. 1).

² To derive the curvature effect, two assumptions are made (see KP00). One is that the Lorentz factor of the outflow is nearly a constant. The other is that the observer frequency should be above the cooling frequency of the emission. As far as the RS emission mentioned here is concerned, these assumptions are satisfied. So we take $(t_\oplus/t_x)^{-(2+p/2)}$ to describe the decline, which has been verified by the detailed numerical calculation (Fan, Wei & Wang 2004; see also Fig. 1 of this work).

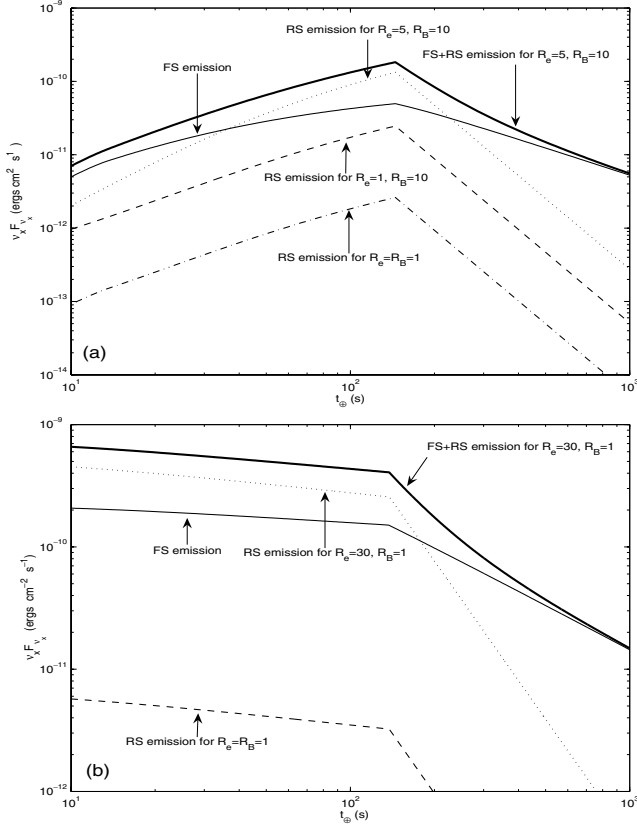


Figure 1. The very early X-ray ($\nu_x = 2.42 \times 10^{17}$ Hz) sample light curves. For the reverse-shock emission component, \mathcal{R}_e and \mathcal{R}_B have been marked in the figure. (a) The ISM model: the parameters are taken to be $n = 1 \text{ cm}^{-3}$, $E_{\text{ISO},53} = 1$, $z = 1$, $\Delta = 6 \times 10^{11} \text{ cm}$, $\epsilon_e^f = 0.1$, $\epsilon_B^f = 0.001$, $\eta = 200$, and $p = 2.4$. (b) The wind case: following P05, we take $A_* = 0.003$, $\epsilon_e^f = 0.01$, $\epsilon_B^f = 0.5$, $E_{\text{ISO},53} = 0.28$, $p = 2.5$, and $z = 0.36$. In addition, we assume $\eta = 200$ and $\Delta = 3.0 \times 10^{12} \text{ cm}$.

2.2 Late internal-shock model

In the standard fireball model of GRBs, the γ -ray emission is powered by internal shocks, the duration of which depends on the active time of the central engine. However, the variability of some GRB afterglows implies that the activity of the GRB central engine may last much longer than the duration of the prompt emission recorded by γ -ray monitors (e.g. Dai & Lu 1998; Granot, Nakar & Piran 2003; Ioka, Kobayashi & Zhang 2005). In addition, it has been proposed that the Fe line observed in some GRB X-ray afterglows could be attributed to prolonged activity of the central engine (Rees & Mészáros 2000; Gao & Wei 2005).

A possible mechanism for the re-activation of the central engine could be as follows. During the accretion phase which powers the prompt γ -ray emission, a fraction of the material constituting the massive progenitor could possibly be pulled out; the central engine could thus be restarted at a later time by the fall back of part of this material on to the central collapsar remnant (King et al. 2005).

Here we assume that the central engine re-starts a few minutes after the prompt γ -ray emission, powering a new unsteady relativistic outflow. We suppose that the Lorentz factor of the ejected material can be highly variable, setting $\Gamma_s \sim 10$ and $\Gamma_f \sim 100$, as the typical Lorentz factors of the slow and fast shells, respectively. The masses of the slow and fast shells are taken as $m_f \simeq m_s$. When an inner fast shell catches up with an outer slow shell at a radius $\sim 2\Gamma_s^2 c \delta t_{\oplus} / (1 + z)$ (where δt_{\oplus} is the observed typical variability

time-scale of the X-ray flares), internal shocks are generated. The Lorentz factor of the merged shell is $\Gamma \approx \sqrt{\Gamma_f \Gamma_s}$ (e.g. Piran 1999), and the Lorentz factor of the internal shocks can be estimated by $\Gamma_{\text{sh}} \approx (\sqrt{\Gamma_f/\Gamma_s} + \sqrt{\Gamma_s/\Gamma_f})/2$. We refer to these re-generated internal shocks as ‘late internal shocks’.

2.2.1 Physical parameters

The internal-shock model has been discussed by many authors (e.g. Paczyński & Xu 1994; Rees & Mészáros 1994; Daigne & Mochkovitch 1998, 2000; Piran 1999; Dai & Lu 2002). Generally speaking, to calculate the synchrotron emission of internal shocks, the following parameters are involved: the outflow luminosity L_m , δt_{\oplus} , Γ , Γ_{sh} , and of course the shock parameters ϵ_e and ϵ_B . For typical GRBs, (L_m , δt_{\oplus} , Γ , Γ_{sh} , ϵ_e , ϵ_B) are taken to be $\sim (10^{52} \text{ erg s}^{-1}$, 0.001–0.01 s, 100–1000, a few, 0.5 and 0.01–0.1), respectively (e.g. Dai & Lu 2002).

The time-averaged isotropic luminosity (2–700 keV) of the X-ray re-bursting of GRB 01121 is $L_x \sim 6 \times 10^{48} \text{ erg s}^{-1}$ (P05). So we normalize our expression by taking $L_m \sim 5 \times 10^{49} L_{x,49} (\epsilon/0.2)^{-1} \text{ erg s}^{-1}$, where ϵ is the efficiency factor of the X-ray flare. We take $\epsilon \sim 0.2$, as found in typical GRBs/XRFs (Lloyd-Ronning & Zhang 2004). Such small L_m (comparing with the GRB case) implies that the fallback accretion rate is just ~ 0.001 – 0.01 times that of the prompt accretion, if the efficiency factor of converting the accretion energy into the kinetic energy of the outflow is nearly a constant (MacFadyen, Woosley & Heger 2001).

The δt_{\oplus} measured in X-ray flares is significantly longer than that measured in the intrinsic hard burst (Burrows et al. 2005). In this Letter, we take $\delta t_{\oplus} \sim 10$ s. The spectra of the X-ray flares detected so far are all non-thermal. The optically thin condition implies a lower limit on the bulk Lorentz factor of the merged shell (e.g. Rees & Mészáros 1994)

$$\Gamma > 11 L_{m,49.7}^{1/5} [1.36/(1+z)]^{-1/5} \delta t_{\oplus,1}^{-1/5}. \quad (8)$$

The typical radius of the late internal shock is $R_{\text{int}} \approx 2\Gamma^2 c \delta t_{\oplus} / (1+z) > 5 \times 10^{13} \text{ cm } L_{m,49.7}^{2/5} [1.36/(1+z)]^{3/5} \delta t_{\oplus,1}^{3/5}$.

As we will show in the following section, with $L_m \sim 5 \times 10^{49} \text{ erg s}^{-1}$, $\delta t_{\oplus} \sim 10$ s, $\Gamma \sim 30$, $\Gamma_{\text{sh}} \sim 2$, $\epsilon_e \sim 0.5$, and $\epsilon_B \sim 0.1$, most of the internal shock’s energy is emitted in the soft X-ray band and the predicted flux matches the observation of the X-ray flare in GRB 01121. Alternatively, as shown in Barraud et al. (2005), with $\epsilon \sim 0.01$ (correspondingly, $L_m \sim 10^{51}$ – $10^{52} \text{ erg s}^{-1}$ and $\Gamma_{\text{sh}} \sim 1.06$), $\delta t_{\oplus} \sim$ a few seconds, and $\Gamma \sim$ a few hundred, X-ray dominated luminosity is expected, too. (Please note that their calculation of the internal shocks emission is somewhat different from ours; see Barraud et al. 2005 for details). Therefore, we believe that with proper parameters, X-ray flares do appear in the late internal-shocks scenario.

2.2.2 The synchrotron radiation of ‘late internal shocks’

Following Dai & Lu (2002), the comoving number density of the unshocked outflow is estimated by $n_e \approx L_m / (4\pi \Gamma^2 R_{\text{int}}^2 m_p c^3)$, where m_p is the rest mass of a proton. The thermal energy density of the shocked material is calculated by $e \approx 4\Gamma_{\text{sh}}(\Gamma_{\text{sh}} - 1)n_e m_p c^2$ (Blandford & McKee 1977). The intensity of the generated magnetic field is estimated by $B \approx (8\pi \epsilon_B e)^{1/2} \approx 6 \times 10^3 \text{ G } \epsilon_{B,-1}^{1/2} [\Gamma_{\text{sh}}(\Gamma_{\text{sh}} - 1)/2]^{1/2} L_{m,49.7}^{1/2} \Gamma_{\text{int},14.5}^{-1} R_{\text{int},14.5}^{-1}$.

As usual, we assume that in the shock front, the accelerated electrons distribute as $dn_e/d\gamma_e \propto \gamma_e^{-p}$ for $\gamma_e > \gamma_{e,m}$, where $\gamma_{e,m} = \epsilon_e(\Gamma_{\text{sh}} - 1)/[(p - 2)m_p]/[(p - 1)m_e]$ is the minimum Lorentz

factor of the shocked electrons (Sari et al. 1998), and m_e is the rest mass of an electron. In this section, we take $p = 2.5$. The observed typical frequency of the synchrotron radiation reads

$$\begin{aligned} \nu_{m,\oplus} &= \gamma_{e,m}^2 q_e \Gamma B / [2(1+z)\pi m_e c] \\ &\simeq 2.7 \times 10^{16} \text{ Hz } \epsilon_{e,-0.3}^2 \epsilon_{B,-1}^{1/2} (\Gamma_{\text{sh}} - 1)^{5/2} (\Gamma_{\text{sh}}/2)^{1/2} \\ &\quad \times L_{m,49.7}^{1/2} \Gamma_{1.5}^{-2} \delta t_{\oplus,1}^{-1}, \end{aligned} \quad (9)$$

i.e. most of the shock energy is emitted in the soft X-ray band, where q_e is the charge of an electron.

The cooling Lorentz factor is estimated by (e.g. Sari et al. 1998) $\gamma_{e,c} \approx 7.7 \times 10^8 (1+z)/(\Gamma B^2 \delta t_{\oplus})$, and the corresponding cooling frequency reads as

$$\begin{aligned} \nu_{c,\oplus} &= \gamma_{e,c}^2 q_e \Gamma B / [2(1+z)\pi m_e c] \\ &\simeq 10^{10} \text{ Hz } [1.36/(1+z)]^2 \epsilon_{B,-1}^{-3/2} \Gamma_{1.5}^8 \\ &\quad \times [\Gamma_{\text{sh}}(\Gamma_{\text{sh}} - 1)/2]^{-3/2} L_{m,49.7}^{-3/2} \delta t_{\oplus,1}. \end{aligned} \quad (10)$$

The synchrotron self-absorption frequency is estimated by (Li & Song 2004)

$$\nu_{a,\oplus} \simeq 10^{15} \text{ Hz } [1.36/(1+z)]^{3/7} L_{m,49.7}^{2/7} \Gamma_{1.5}^{-5/7} \delta t_{\oplus,1}^{-4/7} B_3^{1/7}. \quad (11)$$

The maximum spectral flux of the synchrotron radiation is (e.g. Wijers & Galama 1999) $F_{\text{max}} \approx 3\sqrt{3}\Phi_p(1+z)N_e m_e c^2 \sigma_T \Gamma B / (32\pi^2 q_e D_L^2)$, where $N_e = L_m \delta t / [(1+z)\Gamma m_p c^2] = 8 \times 10^{51} [1.36/(1+z)] L_{m,49.7} \Gamma_{1.5}^{-1} \delta t_{\oplus,1}$ is the number of electrons involved in the emission. Φ_p is a function of p , for $p = 2.5$, $\Phi_p \approx 0.6$ (Wijers & Galama 1999). For $\nu_{c,\oplus} < \nu_{a,\oplus} < \nu_x < \nu_{m,\oplus}$, the predicted flux is (e.g. Sari et al. 1998)

$$\begin{aligned} F_{\nu_x} &= F_{\text{max}} (\nu_{m,\oplus}/\nu_{c,\oplus})^{-1/2} (\nu_x/\nu_{m,\oplus})^{-p/2} \\ &\approx 2.5 \text{ mJy } [\nu_x/(2.42 \times 10^{17} \text{ Hz})]^{-p/2} \epsilon_{e,-0.3}^{p-1} \epsilon_{B,-1}^{(p-2)/4} \\ &\quad \times (\Gamma_{\text{sh}}/2)^{(p-2)/4} (\Gamma_{\text{sh}} - 1)^{(5p-6)/4} L_{m,49.7}^{(p+2)/4} \Gamma_{1.5}^{2-p} \delta t_{\oplus,1}^{(2-p)/2} D_{L,27.7}^{-2}. \end{aligned} \quad (12)$$

Taking $Q_y = 1$ and $\nu_x = 2.42 \times 10^{17} \text{ Hz}$, with equation (12) we have $F_{\nu_x} \approx 2.5 \text{ mJy}$, which matches the observation of GRB 011121 ($\sim 1 \text{ mJy}$). The V band flux can be estimated as ($\nu_{c,\oplus} < \nu_v < \nu_{a,\oplus}$) $F_{\nu_v} \sim F_{\text{max}} \nu_{a,\oplus}^{-3} \nu_{c,\oplus}^{1/2} \nu_v^{5/2} \sim 40 \text{ mJy}$.

What happens after the ‘late internal shocks’? Surely, the re-freshed relativistic outflow will catch up with the initial outflow when the latter has swept a large amount of material and got decelerated. That energy injection would give rise to a flattening (e.g. Rees & Mészáros 1998) or re-brightening signature (e.g. Panaitescu, Mészáros & Rees 1998; Kumar & Piran 2000; Zhang & Mészáros 2002), which could potentially account for the late re-brightening of XRF 050406, the late X-ray re-bursting detected in GRB 050502b and the second/weaker X-ray bump observed in GRB 011121. However, the detailed light-curve modelling is beyond the scope of this Letter.

2.2.3 The behaviour of the flare in decline

For observer’s frequencies above the cooling frequency, the curvature effect dominates the temporal behaviour of the observed flux after the central engine shuts down at $t_{e,\oplus}$ (PK00). The flux declines as

$$\sum_i F_{\nu_x,i} [(t_{\oplus} - t_{eje,i})/\delta t_{\oplus,i}]^{-(2+p_i/2)}$$

(PK00), where i represents the i th pulse, $t_{eje,i}$ and $t_{\oplus,i}$ are the ejection time and the variability time-scale of the i th pulse, respectively. Such a decline is much steeper than $(t_{\oplus}/t_{e,\oplus})^{-(2+p/2)}$ for $t_{e,\oplus} \gg$

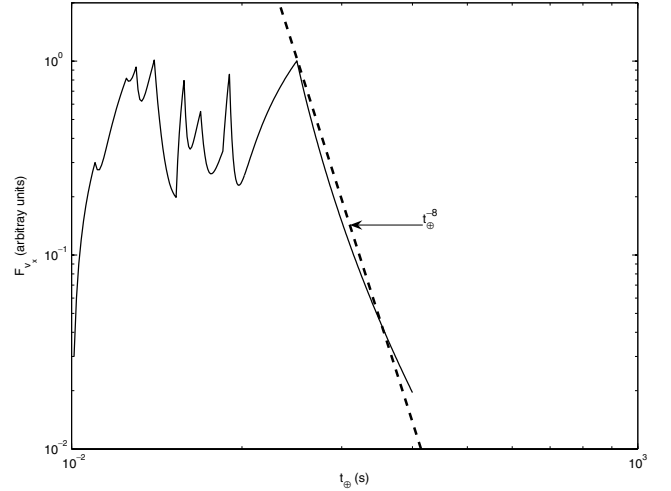


Figure 2. The X-ray light curve of one flare consisting of ten pulses (the solid line, for illustration, each takes the profile $F_{\nu_x} \propto [(t_{\oplus} - t_{eje})/\delta t_{\oplus}]$ for $t_{eje} < t_{\oplus} < t_{eje} + \delta t_{\oplus}$ and $F_{\nu_x} \propto [(t_{\oplus} - t_{eje})/\delta t_{\oplus}]^{-3.25}$ for $t_{\oplus} > t_{eje} + \delta t_{\oplus}$. In these pulses ($i = 1-10$), the peak of $F_{\nu_x,i}$ are taken to be (0.3, 0.8, 0.6, 0.9, 0.1, 0.7, 0.5, 0.3, 0.7, 1.0), respectively (in arbitrary units); $\delta t_{\oplus,i}$ are taken to be (10, 15, 5, 10, 13, 5, 9, 11, 5, 60) s, respectively; $t_{eje,i}$ are taken to be (100, 110, 125, 130, 140, 153, 158, 169, 185, 190) s, respectively. $t_{e,\oplus} \approx t_{eje,10} + \delta t_{\oplus,10} = 250$ s. The dashed line represents $F_{\nu_x} \propto (t_{\oplus}/t_{e,\oplus})^{-8}$.

$\max\{\delta t_{\oplus,i}\}$. For example, as shown in Fig. 2, the decline of the flare is dominated by the curvature effect of the last long pulse with $\delta t_{\oplus} \sim 0.24 t_{e,\oplus}$. A crude power-law fit to the decline yields $F_{\nu_x} \propto (t_{\oplus}/t_{e,\oplus})^{-8}$, which is steep enough to match the sharpest decline detected so far. In reality, the central engine does not turn off abruptly. The dimmer and dimmer emission powered by the weaker and weaker ‘late internal shocks’ may dominate over the curvature effect of the early pulses, resulting in a shallower decay.

3 BEHAVIOUR OF THE X-RAY FLARE IN DECLINE: CONSTRAINT ON THE MODEL

Early X-ray flares have been well detected in GRB 011121, XRF 050406, GRB 050502b and GRB 050730 (P05; Burrows et al. 2005; Starling et al. 2005). The rise and the fall of the first flare (also the dominant one) in GRB 011121 are both very steep. Similar temporal behaviour is evident in other events. The sharp decline of these flares imposes a robust constraint on the model, as shown below.

The X-ray flare detected in GRB 011121 appears at $t_{b,\oplus} = 239$ s and peaks at $t_{p,\oplus} = 270$ s. The burst is believed to be born in a weak stellar wind. As shown in Fig. 1(b), no flare is expected in the FS–RS model. The FS–RS shock model is further disfavoured by its shallow decline. In the late internal-shock model, the decline of the flare can be steep enough to account for the observation (see Fig. 2 for illustration). Moreover, as shown in Section 2.2.2, with proper parameters the observed flux can be well reproduced. So the ‘late internal-shock model’ is favoured. We would like to point out that *the fall of the X-ray flare detected in GRB 011121 is still attributed to the late internal shocks rather than to the curvature effect*. The reason is as follows. Since $\delta t_{\oplus} \leq (t_{p,\oplus} - t_{b,\oplus}) = 31$ s, the resulting decline $F_{\nu_x} \propto [1 + (t_{\oplus} - 270)/\delta t_{\oplus}]^{-3.15}$ is much steeper than the observation $F_{\nu_x} \propto [(t_{\oplus} - 239)/31]^{-1.4}$ (see Fig. 7 of P05) if after $t_{p,\oplus}$ there are no longer any internal shocks.

The X-ray flare detected in XRF 050406 peaks at $t_{p,\oplus} \approx 210$ s and declines as $F \propto t_{\oplus}^{-5.7}$. The X-ray flare detected in GRB 050502b peaks at $t_{p,\oplus} \approx 650$ s and declines as $F \propto t_{\oplus}^{-7}$. In the X-ray afterglow

light curve of GRB 050730, there are three X-ray flares (ranging from 200 to 800 s after the trigger of the GRB). A crude fit to the decline of these three flares results in $F \propto t_{\oplus}^{-5}$ or steeper. Obviously, the FS–RS scenario is ruled out by the steep observed decays and the ‘late internal-shock model’ is favoured. For the X-ray flare detected in GRB 050502b, the late internal-shock model interpretation is further supported by the sharp spike detected in the 1.0–10.0 keV band (Burrows et al. 2005).

4 SUMMARY AND DISCUSSION

In this work, we have explored two possible models which might give rise to X-ray flares in GRB afterglows. One is the external forward-reverse shock model (the ISM model), in which the shock parameters of forward/reverse shocks are taken to be quite different. *The other is the ‘late internal-shock model’, which requires that a refreshed unsteady relativistic outflow is generated after the prompt γ -ray emission* (see Ramirez-Ruiz, Merloni & Rees 2001, for alternative scenarios), *perhaps due to the fallback accretion on to the central collapsar remnant.* The refreshed outflow may be characterized by a low outflow luminosity ($\sim 10^{49}$ erg s $^{-1}$), a small bulk Lorentz factor (~ 30), and a long variability time-scale (~ 10 s). In the external forward-reverse shock model, after the peak of the reverse shock emission ($t_{p,\oplus} = t_x$), the flux can not decline more sharply than $(t_{\oplus}/t_{p,\oplus})^{-(2+p/2)}$ (see Fig. 1). In the ‘late internal-shock model’, the decline can be much steeper than $(t_{\oplus}/t_{c,\oplus})^{-(2+p/2)}$ if the central engine shuts down after $t_{c,\oplus}$ and the longest variability time-scale of the X-ray flare is much shorter than $t_{c,\oplus}$ (see Fig. 2).

For the X-ray flares detected in GRB 011121, XRF 050406, GRB 050502b and GRB 050730, the external forward-reverse shock model is ruled out directly by its shallow temporal decay. For the same reason, other possible external models (i.e. the model related to the external forward shock), including the density jump model, the two-components jet model, the patch jet model and the energy injection model are ruled out as well (Zhang et al. 2005). Thus, the ‘late internal-shock model’ is found to be favoured. In this model, optical emission may be suppressed due to strong synchrotron self-absorption. In the ultraviolet band, however, the radiation could be quite strong. Large amounts of neutral gas would be ionized, as detected in GRB 050502b and GRB 050730 (Burrows et al. 2005; Starling et al. 2005).

Very early X-ray flares are well detected both in long GRBs and in XRFs, which strengthens the correlation of these two phenomena, though the nature of XRFs is still unclear (see Barraud et al. 2005 and references therein).

Finally, we suggest that the early X-ray light curve of some GRBs may be a superposition of the emission powered by the long activity of the central engine and the emission of the external forward shock. As a consequence, the X-ray temporal behaviour may be quite different from that of the long wavelength (UV/optical) emission. This prediction can be tested directly by the UV/Optical Telescope and the X-ray Telescope on board the *Swift* observatory in the near future.

ACKNOWLEDGMENTS

We thank Bing Zhang and E. W. Liang for informing us about Piro et al.’s paper on GRB 011121 at the end of February 2005, and G. F. Jiang, L. J. Gou, Z. Li and H. T. Ma for kind help. We also appreciate the referees for their helpful comments and the third referee for her/his great help. This work is supported by the National Natural Science Foundation (grants 10225314 and 10233010) of

China, and the National 973 Project on Fundamental Researches of China (NKBRF G19990754).

REFERENCES

- Akerlof C. et al., 1999, *Nat*, 398, 400
 Barraud C., Daigne F., Mochkovitch R., Atteia J. L., 2005, *A&A*, in press (astro-ph/0507173)
 Blake C. H. et al., 2005, *Nat*, 435, 181
 Blandford R. D., McKee C. F., 1977, *MNRAS*, 180, 343
 Bloom J. S. et al., 2002, *ApJ*, 572, L45
 Burrows D. N. et al., 2005, *Sci*, 309, 1833
 Dai Z. G., Lu T., 1998, *A&A*, 333, L87
 Dai Z. G., Lu T., 2002, *ApJ*, 580, 1013
 Daigne F., Mochkovitch R., 1998, *MNRAS*, 296, 275
 Daigne F., Mochkovitch R., 2000, *A&A*, 358, 1157
 Fan Y. Z., Dai Z. G., Huang Y. F., Lu T., 2002, *Chin. J. Astron. Astrophys.*, 2, 449
 Fan Y. Z., Wei D. M., Wang C. F., 2004, *A&A*, 424, 477
 Fan Y. Z., Zhang B., Wei D. M., 2005, *ApJ*, 628, L25
 Fox D. et al., 2003, *ApJ*, 586, L5
 Gao W. H., Wei D. M., 2005, *ApJ*, 628, 853
 Garnavich P. M. et al., 2003, *ApJ*, 582, 924
 Granot J., Nakar E., Piran T., 2003, *Nat*, 426, 138
 Greiner J. et al., 2003, *ApJ*, 599, 1223
 Infante L., Garnavich P. M., Stanek K. Z., Wyrzykowski L., 2001, *GCN*, 1152, 1
 Ioka K., Kobayashi S., Zhang B., 2005, *ApJ*, 631, 429
 King A., O’Brien P. T., Goad M. R., Osborne J., Olsson E., Page K., 2005, *ApJ*, 630, L113
 Kobayashi S., 2000, *ApJ*, 545, 807
 Kobayashi S., Zhang B., Mészáros P., Burrows W., 2005, *ApJL*, submitted (astro-ph/0506157)
 Kumar P., Panaitescu A., 2000, *ApJ*, 541, L51 (KP00)
 Kumar P., Panaitescu A., 2003, *MNRAS*, 346, 905
 Kumar P., Piran T., 2000, *ApJ*, 532, 286
 Li Z., Song L. M., 2004, *ApJ*, 608, L17
 Li W. D., Filippenko A. V., Chornock R., Jha S., 2003, *ApJ*, 586, L9
 Lloyd-Ronning N. M., Zhang B., 2004, *ApJ*, 601, 371
 MacFadyen A. I., Woosley S. E., Herger A., 2001, *ApJ*, 550, 410
 McMahon E., Kumar P., Panaitescu A., 2004, *MNRAS*, 354, 915
 Mészáros P., Rees M. J., 1999, *MNRAS*, 306, L39
 Paczyński B., Xu G. H., 1994, *ApJ*, 427, 708
 Panaitescu A., Kumar P., 2004, *MNRAS*, 353, 511
 Panaitescu A., Mészáros P., Rees M. J., 1998, *ApJ*, 503, 314
 Piran T., 1999, *Phys. Rep.*, 314, 575
 Piro L., 2001, *GCN*, 1147, 1
 Piro L. et al., 2005, *ApJ*, 623, 314 (P05)
 Price P. A. et al., 2002, *ApJ*, 572, L51
 Ramirez-Ruiz E., Merloni A., Rees M. J., 2001, *MNRAS*, 324, 1147
 Rees M. J., Mészáros P., 1994, *ApJ*, 430, L93
 Rees M. J., Mészáros P., 1998, *ApJ*, 496, L1
 Rees M. J., Mészáros P., 2000, *ApJ*, 545, L73
 Sari R., Esin A. A., 2001, *ApJ*, 548, 787
 Sari R., Piran T., 1999, *ApJ*, 517, L109
 Sari R., Piran T., Narayan R., 1998, *ApJ*, 497, L17
 Starling R. L. C. et al., 2005, *A&A*, submitted (astro-ph/0508237)
 Wang X. Y., Dai Z. G., Lu T., 2001, *ApJ*, 556, 1010
 Wei D. M., 2003, *A&A*, 402, L9
 Wijers R. A. M. J., Galama T. J., 1999, *ApJ*, 523, 177
 Zhang B., Mészáros P., 2002, *ApJ*, 566, 712
 Zhang B., Kobayashi S., Mészáros P., 2003, *ApJ*, 595, 950
 Zhang B., Fan Y. Z., Dyks J., Kobayashi S., Mészáros P., Burrows D. N., Nousek J. A., Gehrels N., 2005, *ApJ*, submitted (astro-ph/0508321)
 Zou Y. C., Wu X. F., Dai Z. G., 2005, *MNRAS*, 363, 93

This paper has been typeset from a \LaTeX file prepared by the author.